

Sarcomere length measurement permits high resolution normalization of muscle fiber length in architectural studies

Amanda Felder, Samuel R. Ward and Richard L. Lieber*

Departments of Orthopaedic Surgery and Bioengineering, University of California and Department of Veterans Affairs Medical Centers, San Diego, CA 92161, USA

*Author for correspondence at Department of Orthopaedic Surgery, UC San Diego School of Medicine and VA Medical Center, La Jolla, CA 92093-9151, USA (e-mail: rlieber@ucsd.edu)

Accepted 27 June 2005

Summary

The use of sarcomere length to normalize fiber length in architectural studies is commonly practiced but has not been explicitly validated. Using mouse hindlimb muscles as a model system, ankle joints were intentionally set to angles ranging from 30° to 150° and their muscles fixed. Tibialis anterior (TA), extensor digitorum longus (EDL) and soleus muscles were removed and their raw fiber length measured. Sarcomere length was then measured for each fiber length sample and fiber length was normalized to a standard sarcomere length. As expected, raw fiber length was dependent on tibiotarsal angle ($P < 0.0005$ for all muscles, r^2 range 0.22–0.61), while sarcomere length normalization eliminated the joint-angle dependent variation in fiber length ($P > 0.24$, r^2 range 0.001–0.028). Similarly, one-way ANOVA revealed no

significant differences in normalized fiber length among ankle angles for any of the three muscles ($P > 0.1$), regardless of animal size. To determine the resolution of the method, power calculations were performed. For all muscles studied, there was >90% chance of detecting a 15% fiber length difference among muscles and >60% chance of detecting fiber length differences as small as 10%. We thus conclude that the use of sarcomere length normalization in architectural studies permits resolution of fiber length variations of 15% and may even be effective at resolving 10% fiber length variations.

Key words: sarcomere compliance, muscle architecture, modeling, surgery, fiber length, physiological cross-sectional area.

Introduction

An accurate knowledge of skeletal muscle architecture provides an understanding of muscle design and performance (Gans, 1982; Sacks and Roy, 1982), the ability to plan surgical procedures (Fridén and Lieber, 2001; Fridén and Lieber, 2002), and elucidates motor control strategies utilized by the neuromuscular system (Walmsley et al., 1978; Walmsley and Proske, 1981). Undoubtedly, the two most important parameters obtained from architectural studies are physiological cross-sectional area (PCSA in cm^2) and fiber length (L_f in cm). This is because PCSA is a good predictor of maximum tetanic tension (Powell et al., 1984) while L_f predicts maximum velocity and excursion (Bodine et al., 1987), a muscle's most important functional properties.

Physiological cross-sectional area is typically calculated from muscle specimens (see, for example, Lieber et al., 1992), using the equation:

$$\text{PCSA} = (M_m \cos \theta) / \rho L_f, \quad (1)$$

where M_m is muscle mass (g), ρ is muscle density and θ is fiber pennation angle. Alternatively, PCSA may be calculated from

imaging studies (see, for example, Fukunaga et al., 1992), using the equation:

$$\text{PCSA} = V_m / L_f, \quad (2)$$

where muscle volume (V_m in cm^3) is quantified from reconstructed images. In either case, estimates of PCSA rely strongly and nonlinearly on measurements of L_f (because it is in the denominator of both Eq. 1 and 2) and thus it is clear that reliable architectural information depends on obtaining accurate L_f values. One difficulty in obtaining accurate L_f values, is compensating for the natural fiber length variation that occurs simply because muscles are fixed at different joint angles, or because images are obtained with limbs at different joint angles. It is nearly impossible to set joint angles, precisely due to the masking effects of soft tissues that overlie bones (Fig. 1A). Another difficulty is the natural variation in fiber length that occurs within muscles, making it difficult to compare either between muscles or between treatments.

The procedure typically used to standardize L_f values and compensate for such variation is to measure sarcomere length

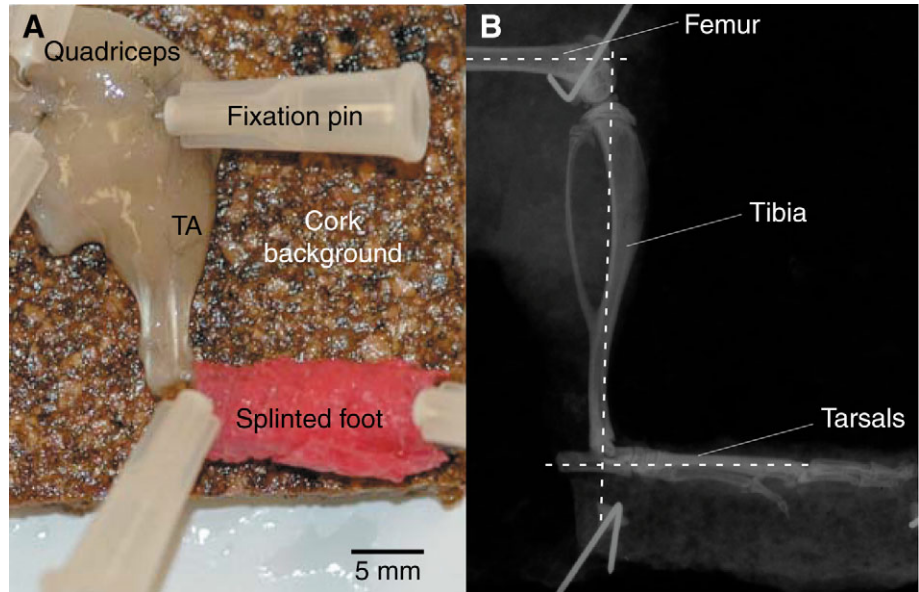


Fig. 1. (A) Photograph of a disarticulated and skinned mouse hindlimb secured to cork for fixation and architectural analysis. Bones are pinned with 30 gauge needles and the foot is secured to a cork footplate that aligns the tarsal and metatarsal bones. In this example, we attempted to fix the limb in 90° of knee flexion and 90° of ankle flexion. TA, tibialis anterior. (B) Lateral radiograph of hindlimb shown in A. Ankle and knee joint angles were as defined as in Materials and methods (shown as dotted lines) and were measured as 89.4° (knee) and 92.4° (ankle).

within a specimen, select a standard sarcomere length, and then normalize all raw fiber lengths using the equation:

$$L_f = L_f' L_s / L_s', \quad (3)$$

where L_f is the normalized fiber length (cm), L_f' is the experimentally measured (raw) fiber length (cm), L_s is a standard sarcomere length (μm) and L_s' is the experimentally measured sarcomere length at the experimentally measured fiber length (μm). This commonly used equation assumes that sarcomere length and fiber length are linearly related. However, other sources of compliance such as Z-disks, myofilaments, tendons and the muscle–tendon junction itself, may compromise this assumption, or the L_f variation may be natural and not associated with sarcomere length. As a result, sarcomere length could change nonlinearly with fiber length. In addition, fast and slow muscle fibers, with varying Z-disk widths and muscle–tendon geometry (Eisenberg, 1983), could differentially affect the validity of this assumption. If any of these assumptions are invalid, it calls into question the use of sarcomere length for normalizing L_f values in architectural studies. These assumptions have not been explicitly tested. Thus, the purpose of this study was to intentionally set identical muscles to different lengths and use the normalization method shown in Eq. 3 to test whether L_f could be accurately normalized with high resolution.

Materials and methods

Hindlimb fixation

Nine adult male mice (strain, 129Sv; mass range, 25–30 g) were weighed and killed by cervical dislocation. Both lower extremities were disarticulated at the hip, skinned and the feet secured to cork with Vetrap bandaging tape (3M Corporation, St Paul, MN, USA) to maintain alignment of the tarsal and digital bones. Limbs were divided into five groups ($N=3\text{--}4/\text{group}$) based on the nominal tibiotarsal angles at

which their ankles were to be fixed: 30°, 60°, 90°, 120° or 150°. The limbs, along with the cork splints, were pinned onto cork to maintain the knee at a nominal angle of 90° of flexion and the ankle at the specified tibiotarsal angle (Fig. 1A). Limb muscles were then fixed in 10% buffered formalin for 48 h and rinsed in 1× phosphate buffered saline (PBS) for 72 h (3 rinses × 24 h/rinse). To determine the actual tibiotarsal and tibiofemoral angles of fixation, lateral radiographs were obtained of the limbs (X-ray System 43805 N; Faxitron X-ray, Palo Alto, CA, USA) at settings of 30 kV for a 45 s exposure, and joint angles digitized (ImageJ, version 1.33, NIH). Tibiotarsal angle was defined as the included angle between the axis of the metatarsals and the line from the center of the distal end of the tibia through the center of the tibial plateau, while tibiofemoral angle was defined as the included angle between the long axis of the femur and the line through the tibia as just described (Fig. 1B). Repeatability of digitization was $\pm 0.41^\circ$ (\pm s.d., $N=3$ repeat measures of 16 tibiotarsal angles and 16 tibiofemoral angles).

Fiber bundle dissection

Tibialis anterior (TA), extensor digitorum longus (EDL), and soleus muscles were removed from the limbs, digested in 15% H_2SO_4 for 30 min to facilitate fiber bundle isolation and stored in 1× PBS at room temperature until fiber bundle dissection. Small fiber bundles (5–50 fibers) were dissected from the whole muscle in 1× PBS under a dissecting microscope using 8–20× magnification (Sacks and Roy, 1982). Special care was taken to remove the entire bundle, from tendon to tendon. At least three bundles were isolated from different regions of each soleus and TA muscle while four bundles were isolated from the EDL, one from each muscle belly (Chleboun et al., 1997). Fiber bundle length was measured under the microscope with a digital caliper to the nearest 0.01 mm. Only fibers that remained straight after

fixation were measured. This criterion excluded soleus muscle bundles fixed at ankle joint angles of 150° since, at this angle, fibers had a distinctly wavy appearance and length could not be reliably measured with calipers. Sarcomere length was measured at three different points along each mounted bundle using laser diffraction as previously described (Lieber et al., 1990). Fibers were used only if at least two useable sarcomere lengths were obtained. Such a criterion was necessary to preclude the possibility of normalizing sarcomere length in damaged muscles, where severe nonhomogeneities can exist (Talbot and Morgan, 1996). This criterion excluded 17 fibers from soleus muscles. In general, diffraction pattern quality from the soleus was poor compared to TA or EDL, as has been previously observed (Burkholder et al., 1994).

Raw fiber lengths were normalized to a standard sarcomere length of $2.5 \mu\text{m}$ (assumed to be mouse muscle optimal sarcomere length; see Walker and Schrodt, 1973) using Eq. 3.

Two separate statistical approaches were used to determine the quantitative effect of sarcomere length normalization. First, raw fiber length was regressed against ankle and knee angle using simple and multiple linear regression to determine whether fiber length varied with either ankle or knee joint angle. Then, the same procedure was performed on normalized fiber length to determine whether this variation was eliminated by the sarcomere length normalization procedure. Next, to quantify the resolution of the normalization procedure, raw and normalized fiber lengths were compared across groups by one-way analysis of variance (ANOVA). Attempted and actual joint angles were compared by one-sampled *t*-test. Resolution of the method was defined based on the statistical power ($1-\beta$) achieved using standard statistical power equations (Sokal and Braumann, 1980). This is because the normalization procedure must still have adequate resolution in experimental studies, even after sarcomere length is accounted for. For all tests,

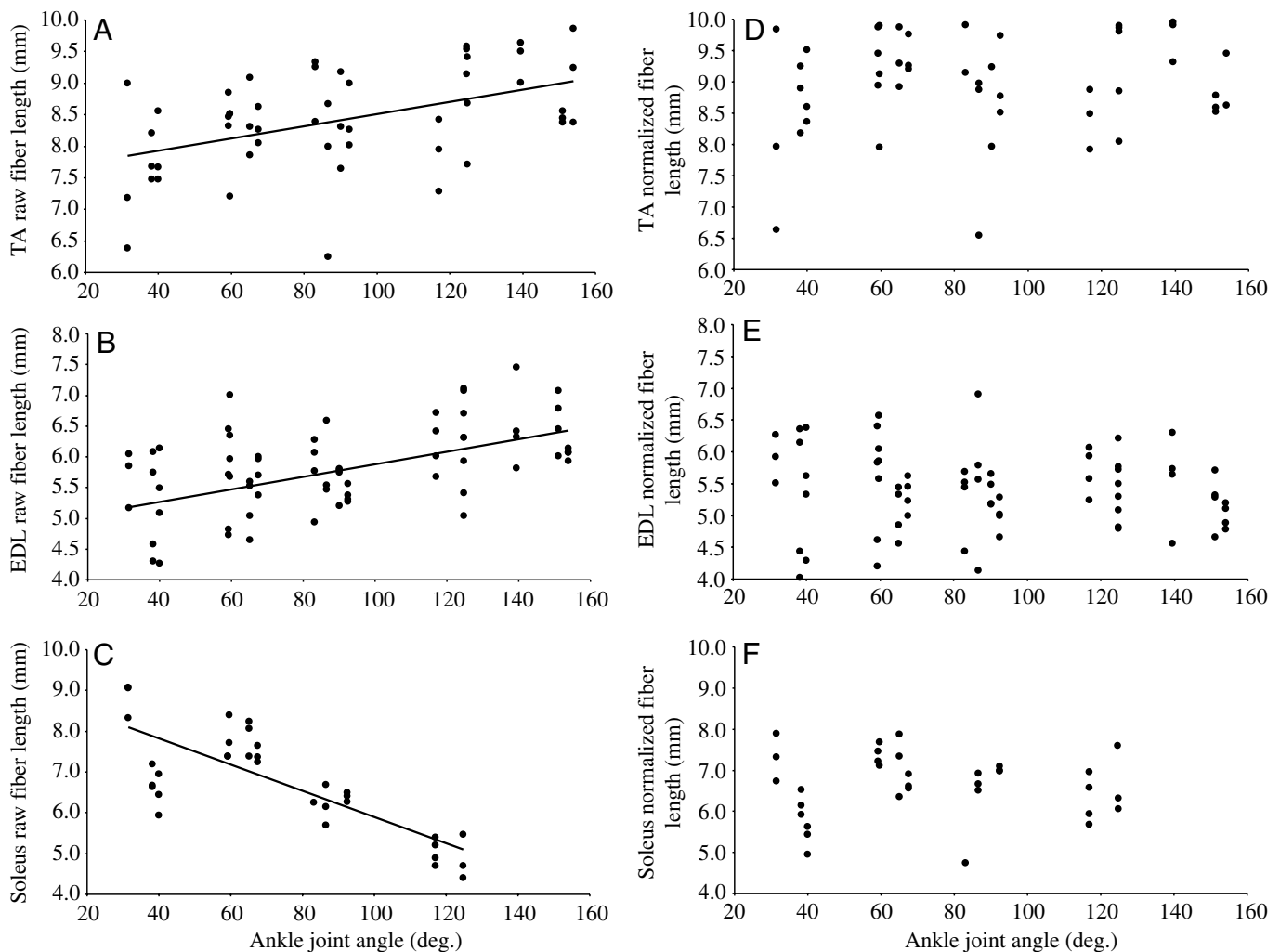


Fig. 2. Relationship between fiber length and joint angle measured radiographically without (A–C) and with (D–F) sarcomere length normalization. (A) Tibialis anterior (TA) raw fiber length vs ankle angle, (B) Extensor digitorum longus (EDL) raw fiber length vs ankle angle, (C) Soleus raw fiber length vs ankle angle, (D) TA normalized fiber length vs ankle angle, (E) EDL normalized fiber length vs ankle angle, (F) Soleus normalized fiber length vs ankle angle. Regression relationships in A, B and C were statistically significant while those in D, E and F were not. See text for details.

critical P -value (α) was set to 0.05 and values are reported in the text as mean \pm S.E.M. unless otherwise noted.

Results and discussion

As anticipated, raw fiber bundle length (referred to as raw fiber length) was strongly dependent on tibiotarsal angle (Fig. 2A–C). As the tibiotarsal angle increased (i.e. as the foot was plantarflexed), TA and EDL fiber length significantly increased (Fig. 2A,B) while soleus fiber length decreased (Fig. 2C; $P < 0.0005$ for all muscles, r^2 range from 0.22–0.61), although the magnitude of the change was muscle-dependent, based on the different fiber length–moment arm relationships of each muscle–joint system (Lieber, 1997).

Variation between intended and actual joint angles was significant for six of the 14 groups of muscles within each intended joint angle ($P < 0.05$). The average joint angle variability around the intended angle was $7.9 \pm 1.4^\circ$ for the knee joint and $4.4 \pm 0.8^\circ$ for the ankle joint. The fact that the variability for the knee was greater probably reflected the greater volume of proximal muscle mass on the femur (Fig. 1A).

Multiple regression analysis revealed that, for the EDL only, raw fiber length was significantly correlated with knee joint angle ($P < 0.05$). This is reasonable based on the fact that the EDL is the only one of the three muscles studied that crosses the knee joint. In spite of this significant correlation, inclusion of knee joint angle in the regression relationship only increased the coefficient of determination marginally (from 0.26 to 0.31). One-way ANOVA results supported regression results in that raw fiber length was significantly different across ankle joint angles for all three muscles ($P < 0.02$).

Sarcomere length normalization effectively eliminated the joint-angle dependent variation in fiber length, evidenced by both linear regression and one-way ANOVA analysis. Linear regression of normalized fiber length on ankle joint angle yielded no significant relationship between the two variables for any of the three muscles (Fig. 2D–F; $P > 0.2$, r^2 range 0.001–0.028), while one-way ANOVA revealed no significant differences in normalized fiber length across all angles for any of the three muscles ($P > 0.1$). This result validates statistically, the use of sarcomere length for fiber length normalization.

A concern in this analysis was that systematic size differences between animals could affect the experimental results. For example, some of the raw fiber length differences between groups could simply reflect animal size. Thus, to determine whether animal size varied significantly among groups, both animal mass and tibial length were compared across groups. Neither animal mass nor tibial length varied significantly among groups, as revealed by one-way ANOVA ($P > 0.5$) and neither were significantly correlated with ankle angle as determined by linear regression (animal mass: $r^2 = 0.008$, $P > 0.7$; tibial length: $r^2 = 0.008$, $P > 0.7$). Thus, animal size did not affect the fiber length analysis presented above.

Having determined that sarcomere length effectively

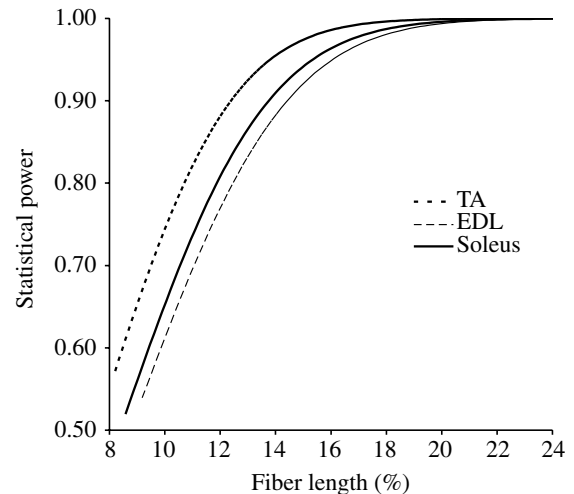


Fig. 3. Relationship between percent fiber length difference detected between groups and statistical power for Extensor digitorum longus (EDL; broken line), soleus (solid line) and Tibialis anterior (TA; dotted line) muscles. These calculations demonstrate that sarcomere length normalization easily permits resolution of fiber length differences of 15%.

normalizes fiber length, a practical consideration becomes defining the resolution of the normalization method. It could be that, due to the large degree of natural variability that occurs in fiber length within muscles fixed at the same joint angle, the lack of significant differences among angles after normalization renders the method imprecise. Note that, in Fig. 2, a great deal of natural fiber length variation occurs within angles that is not eliminated, even after sarcomere length normalization (average within-group coefficient of variation for all muscles at all angles was $11.1 \pm 0.9\%$). This large natural variability is a real phenomenon that has been observed in animal muscles and reported for comparatively large human muscles (Fridén et al., 2001, 2004). Since architectural studies often attempt to define fiber length differences among muscles (see, for example, Lieber et al., 1992) or fiber length changes after surgical intervention (see, for example, Burkholder and Lieber, 1998), it is of interest to determine the ability of such architectural analysis to resolve various relative fiber length differences. This relationship is shown for the EDL, soleus and TA muscles in Fig. 3. The abscissa represents the percentage change in fiber length that could be resolved for a given experiment. As expected, because experimental variability was lowest for the TA muscle, statistical power was highest for this muscle. Both soleus and EDL demonstrate a slight decrease in power at the same relative fiber length difference due to slightly higher intramuscular fiber length variability. Overall, it can be seen that, for all muscles studied, there is $>90\%$ chance of detecting a 15% fiber length difference among muscles and $>60\%$ chance of detecting fiber length differences as small as 10%. We thus conclude that the use of sarcomere length normalization in architectural studies permits resolution of fiber length variations of 15% and may even be effective at resolving 10%

fiber length variations. Of course, this conclusion assumes that fiber length variability in the experimental system chosen is similar to that reported here for the mouse hindlimb. If the variability is much greater than that reported here, it may be necessary to restrict fiber sampling to analogous anatomical regions of muscles or to increase sample size to obtain the same resolving power as presented here.

It should be noted that, while the method of measuring sarcomere length in the current study was laser diffraction, any sarcomere-length measuring approach can be used. This could include phase microscopy of fixed fibers or even paraffin embedding of muscle with longitudinal sectioning of stained tissue. The main point is that sarcomere length must be measured in some way that avoids unnecessary intermuscular variation. The data from Fig. 2 demonstrate that, in the mouse hindlimb system, there is no joint angle at which fiber lengths become 'less variable' such that normalization would become unnecessary. This is supported by the fact that, for all muscles, one-way ANOVA reveals no significant difference among joint angles for coefficient of variation ($P > 0.6$). Alternatively, one might simply try to fix joints at the angle that corresponds to the reference sarcomere length. However, as can be appreciated from Fig. 2, there is no single angle that fulfills this criterion for all muscles, which emphasizes the need for direct sarcomere length normalization.

The authors gratefully the support of the Department of Veterans Affairs and the National Institutes of Health, grants AR40050, AR40539 and HD44822. We appreciate the helpful comments of Drs Jan Fridén and Ilona Barash. We also appreciate the technical assistance of Ms Debbie Trudell.

References

- Bodine, S. C., Roy, R. R., Eldred, E. and Edgerton, V. R.** (1987). Maximal force as a function of anatomical features of motor units in the cat tibialis anterior. *J. Neurophysiol.* **6**, 1730-1745.
- Burkholder, T. J. and Lieber, R. L.** (1998). Sarcomere number adaptation after retinaculum release in adult mice. *J. Exp. Biol.* **201**, 309-316.
- Burkholder, T. J., Fingado, B., Baron, S. and Lieber, R. L.** (1994). Relationship between muscle fiber types and sizes and muscle architectural properties in the mouse hindlimb. *J. Morphol.* **220**, 1-14.
- Chleboun, G. S., Patel, T. J. and Lieber, R. L.** (1997). Skeletal muscular architecture and fiber type distribution with the multiple bellies of the mouse extensor digitorum longus muscle. *Acta Anat. (Basel)* **159**, 147-155.
- Eisenberg, B. R.** (1983). Quantitative ultrastructure of mammalian skeletal muscle. In *Skeletal Muscle* (ed. L. D. Peachey, R. H. Adrian, S. R. Geiger, and M. D. Baltimore), pp. 73-112. Bethesda, MD, USA: American Physiological Society.
- Fridén, J. and Lieber, R. L.** (2001). Quantitative evaluation of the posterior deltoid-to-triceps tendon transfer based on muscle architectural properties. *J. Hand Surg.* **26A**, 147-155.
- Fridén, J. and Lieber, R. L.** (2002). Mechanical considerations in the design of surgical reconstructive procedures. *J. Biomech.* **35**, 1039-1045.
- Fridén, J., Albrecht, D. and Lieber, R. L.** (2001). Biomechanical analysis of the brachioradialis as a donor in tendon transfer. *Clin. Orthop. Relat. Res.* **383**, 152-161.
- Fridén, J., Lovering, R. M. and Lieber, R. L.** (2004). Fiber length variability within the flexor carpi ulnaris and flexor carpi radialis muscles: implications for surgical tendon transfer. *J. Hand Surg.* **29A**, 909-914.
- Fukunaga, T., Roy, R. R., Shellock, F. G., Hodgson, J. A., Day, M. K., Lee, P. L., Kwong, F. H. and Edgerton, V. R.** (1992). Physiological cross-sectional area of human leg muscles based on magnetic resonance imaging. *J. Orthop. Res.* **10**, 928-934.
- Gans, C.** (1982). Fiber architecture and muscle function. *Exerc. Sport Sci. Rev.* **10**, 160-207.
- Lieber, R. L.** (1997). Muscle fiber length and moment arm coordination during dorsi- and plantarflexion in the mouse hindlimb. *Acta Anat. (Basel)* **159**, 84-89.
- Lieber, R. L., Fazeli, B. M. and Botte, M. J.** (1990). Architecture of selected wrist flexor and extensor muscles. *J. Hand Surg.* **15A**, 244-250.
- Lieber, R. L., Jacobson, M. D., Fazeli, B. M., Abrams, R. A. and Botte, M. J.** (1992). Architecture of selected muscles of the arm and forearm: anatomy and implications for tendon transfer. *J. Hand Surg.* **17A**, 787-798.
- Powell, P. L., Roy, R. R., Kanim, P., Bello, M. and Edgerton, V. R.** (1984). Predictability of skeletal muscle tension from architectural determinations in guinea pig hindlimbs. *J. Appl. Physiol.* **57**, 1715-1721.
- Sacks, R. D. and Roy, R. R.** (1982). Architecture of the hindlimb muscles of cats: functional significance. *J. Morphol.* **173**, 185-195.
- Sokal, R. R. and Braumann, C. A.** (1980). Significance tests for coefficients of variation and variability profiles. *Syst. Zool.* **29**, 50-66.
- Talbot, J. A. and Morgan, D. L.** (1996). Quantitative analysis of sarcomere non-uniformities in active muscle following a stretch. *J. Muscle Res. Cell Motil.* **17**, 261-268.
- Walker, S. M. and Schrodt, G. R.** (1973). Segment lengths and thin filament periods in skeletal muscle fibers of the rhesus monkey and humans. *Anat. Rec.* **178**, 63-82.
- Walmsley, B. and Proske, U.** (1981). Comparison of stiffness of soleus and medial gastrocnemius muscles in cats. *J. Neurophysiol.* **46**, 250-259.
- Walmsley, B., Hodgson, J. A. and Burke, R. E.** (1978). Forces produced by medial gastrocnemius and soleus muscles during locomotion in freely moving cats. *J. Neurophysiol.* **41**, 1203-1216.